

***In situ* fibrillation of poly(trimethylene terephthalate) in polyolefin elastomer through multistage stretching extrusion**

Jiahao Dong,^{1,2} Yuanhui Qi,^{1,2} Jing Sun,¹ Liangqiang Wei,¹ Shuhao Qin^{1,2}

¹National Engineering Research Center for Compounding and Modification of Polymer Materials, Guiyang, 550014, China

²Department of Polymer Materials and Engineering, College of Materials and Metallurgy, Guizhou University, Guiyang, 550025, China

Correspondence to: S. Qin (E-mail: qinshuhao@126.com)

ABSTRACT: Polyolefin elastomer (POE)/poly(trimethylene terephthalate) (PTT) microfibrillar composites (MFCs) were successfully fabricated by multistage stretching extrusion with an assembly of laminating-multiplying elements (LMEs). The morphologies of these novel materials were greatly influenced by the compositions. The number of microfibrils increased with increasing PTT concentration, as revealed by scanning electron microscopy. The tensile strength was the highest along the extrusion direction at the weight ratio of 85/15. Moreover, dynamic rheological results showed that the storage modulus, loss modulus, and complex viscosity were the highest while the $\tan \delta$ was the lowest for MFCs prepared at the weight ratio 85/15 compared with the neat POE, especially at low frequency ($\omega < 1$ rad/s). In addition, the PTT microfibrils had more effect on the rheological properties compared to the PTT particles. However, the differences became negligible at high frequency ($\omega > 100$ rad/s). © 2016 Wiley Periodicals, Inc. *J. Appl. Polym. Sci.* **2016**, *133*, 43797.

KEYWORDS: composites; elastomers; mechanical properties; morphology; rheology

Received 22 August 2015; accepted 15 April 2016

DOI: 10.1002/app.43797

INTRODUCTION

Microfibrillar composites (MFCs) are increasingly attracting the interest of researchers.^{1–4} They are usually manufactured from two thermoplastics with different melting temperatures (T_m). The polymer with lower T_m is used as matrix and is reinforced by fibrils of the other polymer with higher T_m (dispersed phase), which are generated *in situ* during processing. Typically, thermoplastic liquid-crystal polymers (TLCP) are used as the dispersion phase to prepare the MFCs and can strengthen the thermoplastic polymer (TP)⁵ because the rodlike TLCP molecules can be oriented, and the reinforcement is achieved *in situ* in the TP matrix.^{6–9} However, the TLCPs are restricted in general engineering applications because of their high price and high processing temperature, so researchers have focused on other polymers, especially engineering polymers like polyamide (PA), poly(ethylene terephthalate) (PET), and so on.

A conventional composite reinforced by fibers (e.g., glass fiber or carbon fiber) is typically an organic–inorganic system and has some unavoidable drawbacks, such as inhomogeneous mixing, high material and labor costs, and environmental unfriendliness. Compared with conventional composites, the MFCs, which are organic–organic systems, have lots of advantages.^{10,11} For example, during the blending of two polymers, the dispersed phase can be achieved more uniformly and the interfacial tension can be

higher, compared with the organic–inorganic blending. Besides, the required equipment is simpler and the manipulation is more convenient. Recently, recycled LCP¹² and PET¹³ were successfully used to reinforce polyolefins, which is a good way to utilize recycled plastics effectively. Moreover, conductive polymer materials were manufactured through multistage stretching extrusion, and conductive particles (carbon black) were assembled within the microfibrils.¹⁴ It is very meaningful to develop a new method to manufacture a functional composite material.

The preparation methods of MFCs can generally be divided into three steps^{15–17}: mixing, fibrillization, and cooling. First of all, the processing temperature should be higher than the melting temperatures of the component polymers to make sure the polymers are melted and blended sufficiently. When a polymer melt flows through an exit die, the matrix and the dispersed phase can be well oriented by the drawing and internal shearing. Finally, the polymers are quenched quickly to preserve the microfibrillar morphology after exiting the extrusion die. In addition, injection molding or compression molding of the MFCs at temperatures between the melting points of the constituent polymers were employed by some researchers. The aim of the above processing is to create an isotropic matrix in which randomly oriented microfibrils are distributed as a dispersed phase.

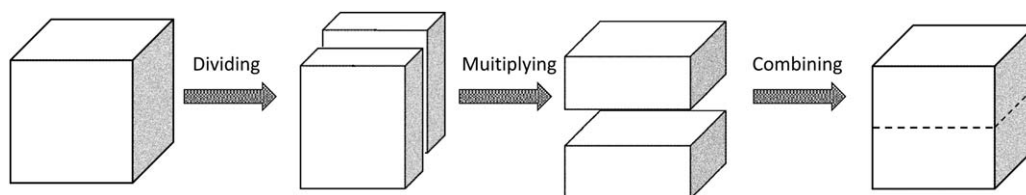


Figure 1. Scheme showing the polymer melt flow process in a laminating-multiplying element (LME).

Recently, an extrusion die with an assembly of laminating-multiplying elements (LMEs) has been attracting our interest. The extrusion die can provide strong shearing and elongational forces. These LMEs have been used to prepare multilayered polymer materials,^{18–20} and some researchers began to use LMEs to prepare MFCs.^{21,22} In this work, when the polymer melt flows through the die, the laminating-multiplying process in each LME can induce stronger shearing and stretching stress on the melt, so the dispersed phase can be easier to deform and become microfibrillar. The schematic of a laminating-multiplying element (LME) is shown in Figure 1, and more details on LMEs are illustrated in refs. 18 and 19.

To the best of our knowledge, studies using polyolefins (mainly polyethylene (PE) and polypropylene (PP)) as the matrix of the MFCs while choosing a thermoplastic elastomer (TPE) as the dispersed phase are rarely reported. In this study, polyolefin elastomer (POE) was chosen as the composite matrix, and poly(trimethylene terephthalate) (PTT), one of the most important materials for engineering plastics and textile fibers, was used as the dispersed phase. The idea in this paper is different from using crosslinking or the addition of a reinforcing filler to enhance the mechanical properties of POE. There are many factors in the extrusion process that may influence the properties of MFCs, such as the viscosity ratio,^{23–26} blend ratio,^{27–29} shear rate,^{30,31} and draw ratio.^{15,32,33} Given that the blend ratio of POE and PTT is one of the most important factors, the influences of the composition on the microfibrillar morphology and the tensile strength of the *in situ* microfibrillar POE/PTT blend were investigated. The number of microfibrils increased with increasing PTT concentration. The tensile strength is the highest along the extrusion direction at the weight ratio 85/15. The dynamic rheological properties are sensitive to the morphology of PTT in the POE matrix, so the dynamic rheological properties were studied, too. The storage modulus, the loss modulus, and the complex viscosity were the highest while the $\tan \delta$ was the lowest for MFCs prepared at a weight ratio of 85/15 compared with the neat POE and the common blends at low frequency ($\omega < 1$ rad/s), but at high frequency ($\omega > 100$ rad/s), the differences became negligible.

EXPERIMENTAL

Materials

The polymers used in this work are POE (ENGAGE 8200) and PTT (Sorona 3301 NC010). The POE (density = 0.870 g/cm³ and melt index (MI) = 5.0 g/10 min at 190 °C) was purchased from Dow Chemical Company (Michigan, USA). The PTT used as the dispersed phase, with a density of 1.32 g/cm³, was pro-

duced by the DuPont Company (Delaware, USA). The melting points of POE and PTT are 59 °C and 228 °C, respectively.

Specimen Preparation

First, PTT was dried in a vacuum oven at 120 °C for 4 h, then the POE/PTT composites with weight ratios of 100/0, 95/5, 90/10, 85/15, and 80/20 were extruded by the homemade multi-stage stretching extrusion assembly, which contains a twin-screw extruder (SHJ-30, Nanjing Jieya Extrusion Equipment Co., Nanjing, China, diameter of screw = 30 mm, length/diameter = 40/1), a water cooling block, and five LMEs. The screw speed was 160 rpm, and the temperatures from the hopper to the exit of the extruder were 220, 235, 240, and 240 °C. In addition, the temperature of LMEs was 240 °C to make sure the POE matrix and PTT dispersed phase were melted and blended sufficiently. When the polymer melt flowed through the LMEs, the laminating-multiplying process in each LME provided strong shearing and stretching stress so the dispersed phase can be deformed and become microfibrils. Finally, the composites went through the water-cooling block to preserve the generated PTT microfibrils. Figure 2 shows the schematic diagram of the multi-stage stretching extrusion system. For comparison, the common POE/PTT composites were extruded by a twin-screw extruder (CTE-20, Nanjing Jieya Extrusion Equipment Co., Nanjing, China, diameter of screw = 20 mm, length/diameter = 40/1). The temperature parameters were the same as the microfiber composites, and the screw speed was 300 rpm.

Scanning Electron Microscopy (SEM)

SEM was used to examine the morphology of the POE/PTT composites. Some samples were quenched in liquid nitrogen and cryofractured along the extrusion direction or the vertical direction. Other samples were immersed in hot xylene for 12 h to etch the POE matrix away. The measurements were done using a Quanta 250 FEG SEM (FEI, Hillsboro, USA) at an accelerating voltage of 10 kV. The diameter distributions were obtained based on 100 microfibrils, and the averaged diameters were calculated as follows:

$$D_N = \frac{\sum N_i D_i}{\sum N_i} \quad (1)$$

where D_N is the number of averaged diameters, and N_i is the number of microfibrils with a diameter of D_i .

Tensile Testing

Tensile tests were performed using an MTS CMT6104 tension machine (Shanghai, China) at a rate of 500 mm/min with an experimental temperature of 23 °C in accordance with ISO 37-2005. At least five specimens for each product were tested, and the average value was calculated.

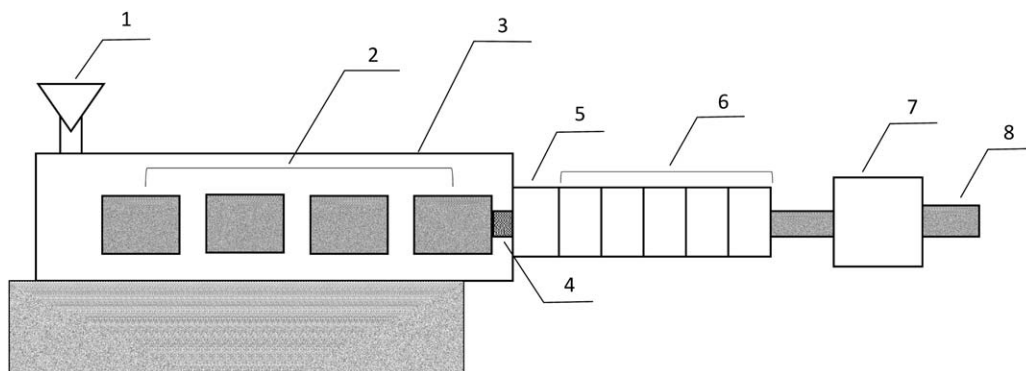


Figure 2. Scheme of the multistage stretching extrusion system: (1) hopper; (2) heating section; (3) twin-screw extruder; (4) exit die; (5) connector; (6) laminating-multiplying elements; (7) water cooling block; (8) sample.

Dynamic Rheological Analysis (DRA)

Dynamic rheological measurements were performed on a rotational rheometer (ARES-G2, TA Instruments, New Castle, USA), employing a parallel-plate sensor with a diameter of 25 mm. The dynamic viscoelastic properties are determined with frequencies from 0.1 to 500 rad/s, using a 5% strain value determined with a stress sweep to stay within the linear viscoelastic region. Measurements were carried out at 200 °C to keep the PTT phase in a solid state.

RESULTS AND DISCUSSION

Morphology Observation

Figure 3 shows the morphologies of the frozen-fractured surface of the POE/PTT common blends (CBs) (weight ratio: 85/15) along the extrusion direction and the vertical direction. The morphology conforms to a typical incompatible system, which is similar to the PE/PET unstretched blends prepared by Li *et al.*¹⁷ Spherical PTT particles are clearly observed, and there is no phase orientation in the shape of the dispersed particles. Moreover, there is no interfacial interaction or adhesion between the PTT and POE since the phase domains of PTT particles are clear and the interfaces are smooth. Considering PTT is a polar polymer while POE is nonpolar, it is reasonable to

deduce that PTT is not only thermodynamically immiscible but also technologically incompatible with POE.

Figure 4 shows the morphology of the frozen-fractured surface of the POE/PTT MFCs with different concentrations of PTT along the extrusion direction and the vertical direction. It is easy to see that the number of PTT microfibrils increased when the concentration of PTT increased. When the concentration of PTT was low, the PTT particles were not uniform. For example, in the POE/PTT (weight ratio: 95/5) composites, the PTT particles are relatively scattered, and the diameters are quite small, so the PTT particles are difficult to deform under the action of shear and stretching. Consequently, some particles appear in the form of fibers with a comparatively small length–diameter ratio, and others are ellipsoid. When the concentration of PTT is increased, the high shear and drawing make the small particles coalesce, and the PTT particles become moderate in size and more easily form microfibrils. Thus, more and more PTT particles become microfibrils, while the number of ellipsoid particles decreases. Figure 4(e–h) shows that most of the PTT microfibrils are broken by the fracture, and only the ends can be seen. In addition, some PTT fibers are pulled out. Some long microfibrils parallel to the cross section are clearly observed in Figure 4, which proves that the PTT particles are

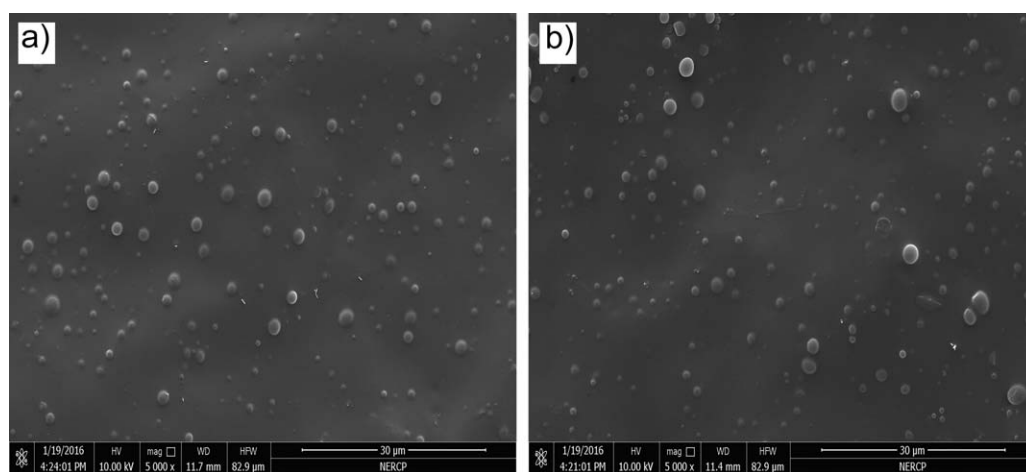


Figure 3. The disperse phase morphology in POE/PTT (weight ratio: 85/15) common blends along different directions: (a) extrusion direction; (b) vertical direction.

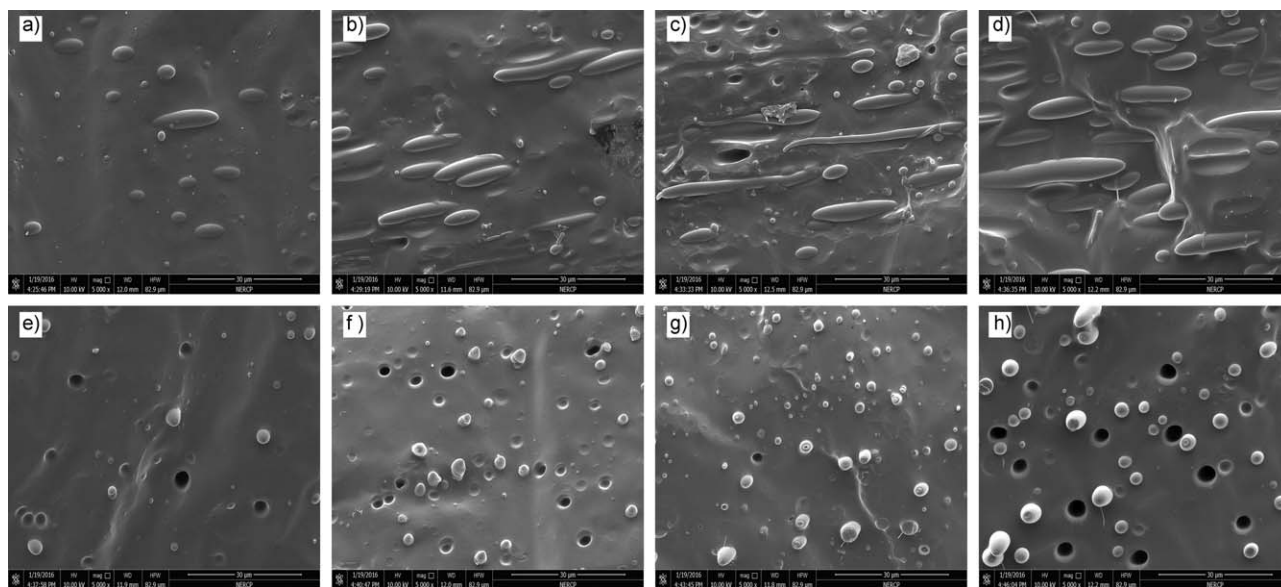


Figure 4. The disperse phase morphology in POE/PTT composites along the extrusion direction (a–d) and the vertical direction (e–h). The weight ratios of POE/PTT are (a), (e) 95/5; (b), (f) 90/10; (c), (g) 85/15; (d), (h) 80/20.

deformed, oriented, and changed into microfibrils under the influence of the high shear and drawing.

Figure 5 shows the morphology of the PTT microfibrils after the dissolution of POE. The diameter distributions of long PTT microfibrils are shown in Figure 6. During the melt blending of polymers, the PTT phase is subjected to breakup and coalescence. The breakup occurs due to the viscous drag force exerted by the POE phase on the PTT phase. The coalescence results from the impingement of PTT droplets because of their intrinsic normal force. When the PTT content is at a low level, the PTT particles are relatively scattered and the diameters are quite small, giving them little chance to coalesce. As a consequence, the PTT particles more easily form the short rods than the long fibers. This can be confirmed in the case of the POE/PTT (95/5) composite, in which a number of PTT particles appear in the form of ellipsoids, and only a few microfibrils with an average diameter of $0.81\ \mu\text{m}$ can be observed. When the PTT content increases, the small particles have more chance to coalesce, and the sizes of the PTT particles become moderate, which more easily form microfibrils, consequently leading to more microfibrils. It is found that both the diameter and length of the microfibrils increase with increasing PPT content. The diameter distributions of PTT microfibrils (for PTT contents of 5%, 10%, and 15%) are relatively uniform, which is good for reinforcing the POE. In contrast, the diameter distribution of microfibrils in the POE/PTT (80/20) composites is wider because of the presence of some large fibrils.

Tensile Testing

The tensile strength and elongation at break of the POE/PTT microfibrillar composites along the extrusion direction and the vertical direction in the weight ratios of 100/0, 95/5, 90/10, 85/15, 80/20 for the POE/PTT system are shown in Figure 7. It can be seen that the tensile strength of the microfibrillar POE/PTT composites decreases a little in the weight ratio of 95/5, while

the reinforcement of the microfibrillar POE/PTT composites is noticeable in the weight ratios of 90/10 and 85/15 along the extrusion direction. For example, the tensile strength of POE is greatly increased from 19.6 to 23.0 MPa when 15% of PTT is added, but when the PTT concentration is 20%, there is a large decrease in the tensile strength. In addition, the elongation at break decreased at first and then increased along the extrusion direction when the content of PTT was increased from 0% to 20%. The minimum value of the elongation at break appears at the weight ratio of 85/15, which has the maximum tensile strength. The elongation at break decreases with the increase of PTT concentration along the vertical direction.

The morphology of the blends affects the mechanical properties strikingly.³⁰ The incompatibility between the PTT phase and the POE matrix is a main factor that hinders the improvement of the composites' properties. Although PTT microfibrils are helpful in reinforcing the mechanical properties, the uniformity of the microfibrils should not be ignored. When the PTT content is comparatively low, the reinforcement is unclear because the microfibril content is fairly low. When the PTT concentration is higher, more microfibrils are formed and the reinforcing effect is improved. The most remarkable point occurs when 15% of PTT is added to the POE matrix, where PTT is almost formed into microfibrils. The diameter distributions of PTT microfibrils are uniform, so this composite had the most significant tensile properties. However, when the PTT content is increased to 20%, more microfibrils can be seen, which causes more potential problems of incompatibility. Moreover, the microfibril distribution of the POE/PTT (80/20) composites is more scattered, which was not helpful in reinforcement. This explains why the addition of 20% PTT reduces the tensile properties of the composite compared to the composite with 15% PTT.

Furthermore, with the increase of PTT concentration, the tensile strength along the vertical direction decreases. This suggests that

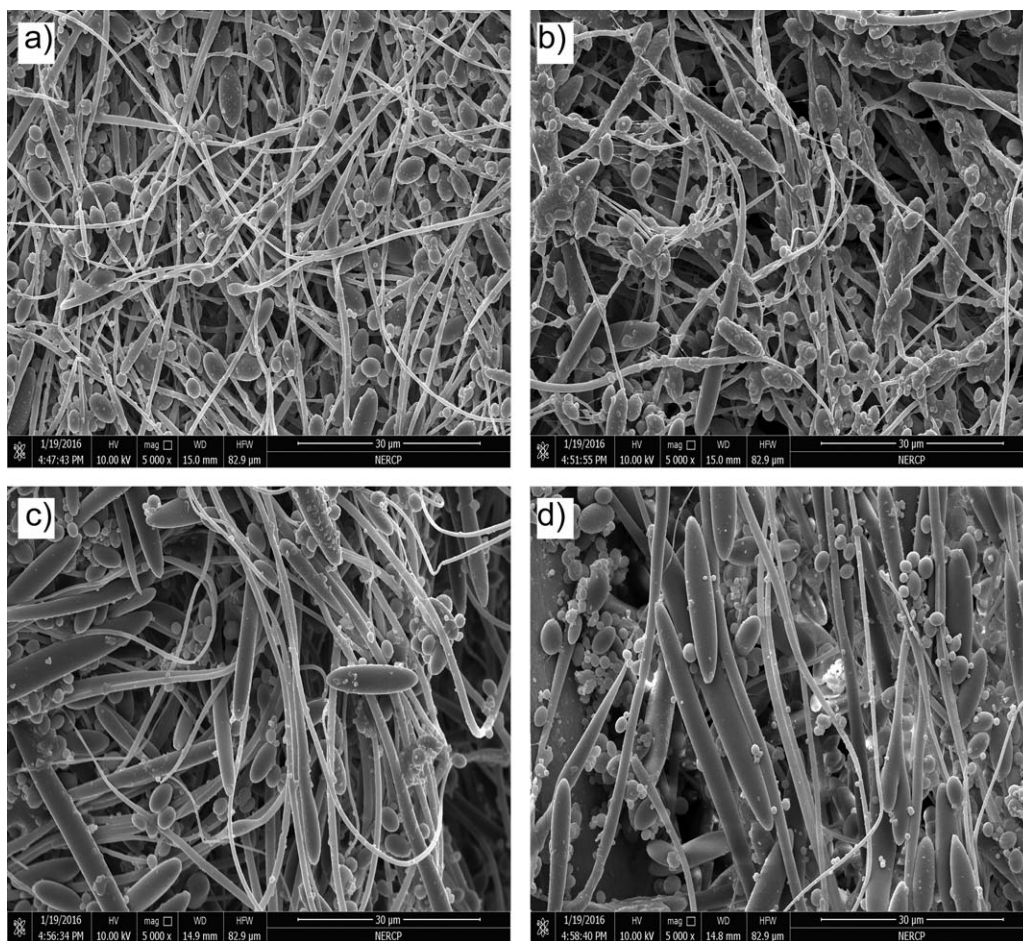


Figure 5. Morphology of the PTT microfibers after the dissolution of POE. The weight ratios of POE/PTT are (a) 95/5; (b) 90/10; (c) 85/15; (d) 80/20.

the PTT microfibrils are more helpful to the tensile strength along the extrusion direction than along the vertical direction. It is reasonable that the PTT particles were oriented and formed microfibers along the extrusion direction under the influences of shear and stretching, and the PTT microfibers do little to improve the compatibility between PTT and POE along the vertical direction.

Dynamic Rheology

Generally, dynamic rheology is sensitive to the filler morphology in a polymer matrix.³³ It is very necessary to investigate the influence of the morphology of the PTT dispersed phase in the POE/PTT composites. The MFCs and the CBs were prepared by the different methods mentioned in the experimental section. The POE/PTT MFCs were prepared through multistage stretching extrusion with five LMEs, and the POE/PTT CBs were extruded by the twin-screw extruder.

The dependence of the storage modulus (G') and the loss modulus (G'') on the PTT content and processing methods are shown in Figure 8 and Figure 9 for the POE/PTT blends, respectively. It is evident from the curves that the G' values and the G'' values of all the specimens increased with increasing angular frequency. The G' values and the G'' values of the POE/PTT MFCs during the test frequency range indicate that 85/

15 > 80/20 > 90/10 > 95/5 > 100/0 [Figures 8(a) and 9(a)]. These results are attributed to the different morphologies and concentrations of the PTT dispersed phase in the POE matrix. The dynamic rheological experiments are implemented at 200 °C. At this temperature, the PTT phase is still in a solid state, while the POE matrix has been melted. Hence, compared with the viscoelastic nature of POE, the PTT phase is stiff. Furthermore, the PTT microfibrils are preserved in the POE matrix, which can contribute in imparting stiffness to the composites. The probability of entanglement between the macromolecular chains in the POE matrix and the microfibrils is much higher when the microfibril content is higher. Hence, both the storage modulus and loss modulus are enhanced simultaneously with an increase in the concentration of the PTT microfibrils. The POE/PTT (80/20) composites have lower G' and G'' values than the POE/PTT (85/15) composites, especially at low frequencies ($\omega < 1$ rad/s), which may be connected with the incompatibility of PTT and POE and the scatter of microfibril distribution in the POE/PTT (80/20) composites.

Moreover, the G' values of the POE/PTT MFCs have more obvious changes than the G'' values at low frequency ($\omega < 1$ rad/s) [Figures 8(a) and 9(a)]. This indicates that the microfibril morphology of the PTT dispersed phase has a more prominent effect on the elastic behavior than on the viscous behavior.

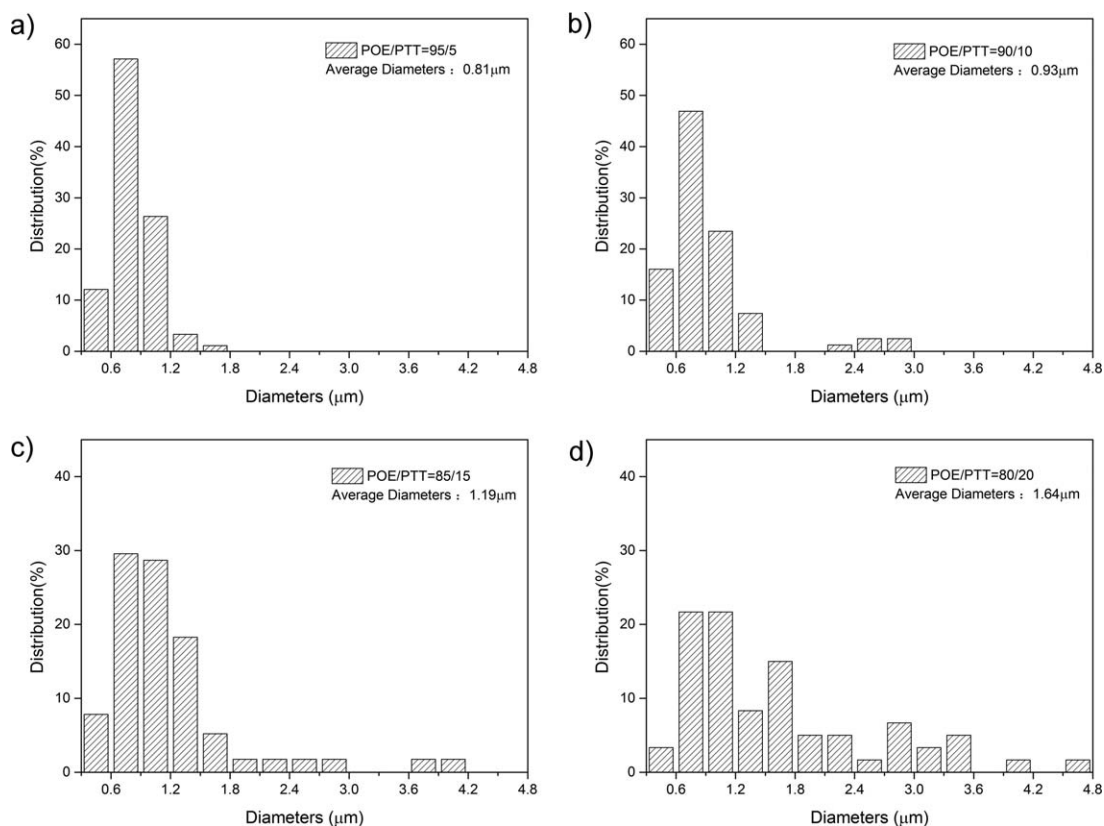


Figure 6. Diameter distributions of PTT microfibrils. The weight ratios of POE/PTT are (a) 95/5; (b) 90/10; (c) 85/15; (d) 80/20.

This is similar to the research of polyethylene (PE)/polycarbonate (PC) *in situ* microfibrillar composites, which were fabricated through multistage stretching extrusion with different LMEs by Wang *et al.*²² Figures 8(b) and 9(b) show that the G' values and the G'' values of the neat POE are similar no matter the processing method. However, at the same PTT concentration (15%), the G' values and the G'' values of MFCs are higher than that of the CBs at the same angular frequency (ω), which can be attributed to the morphology of the dispersed phase. There are many PTT microfibrils in the MFCs, while only PTT spherical particles can be seen in the CBs, which means that PTT microfibrils

make more contributions to both the elastic behavior and the viscous behavior than the PTT particles do.

Tan δ is the ratio of loss modulus to the storage modulus (G''/G'). For higher tan δ values, the rheological behavior of the composites is more like a liquid. Figure 10 shows the angular frequency (ω) dependence of tan δ for the POE/PTT composites at 200 °C. It is found that the tan δ values decrease dramatically with angular frequency (ω) for all the samples except the POE/PTT (85/15) composites [Figure 10(a)]. Even at low frequency ($\omega < 1$ rad/s), there is a plateau region in the tan δ curve. Jayanarayanan *et al.*³³ observed a similar phenomenon in

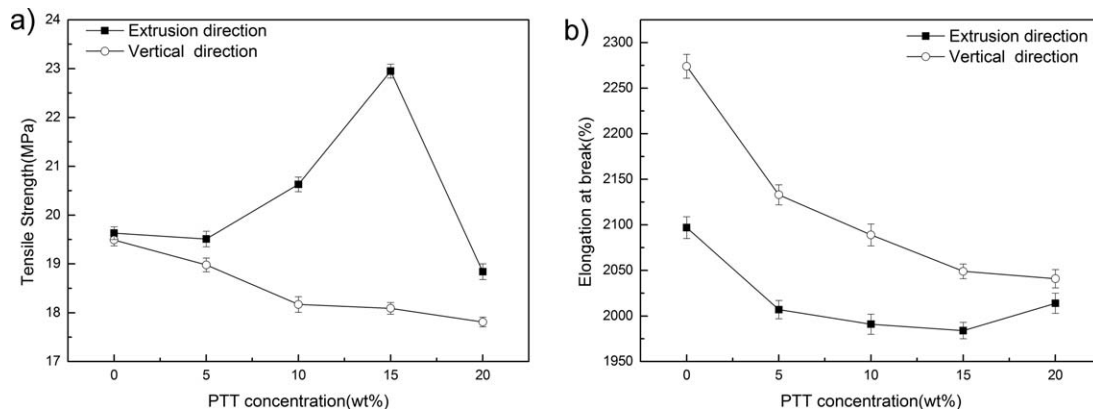


Figure 7. (a) The tensile strength of POE/PTT *in situ* microfibrillar composites along the extrusion direction and the vertical direction. (b) The elongation at break of POE/PTT *in situ* microfibrillar composites along the extrusion direction and the vertical direction.

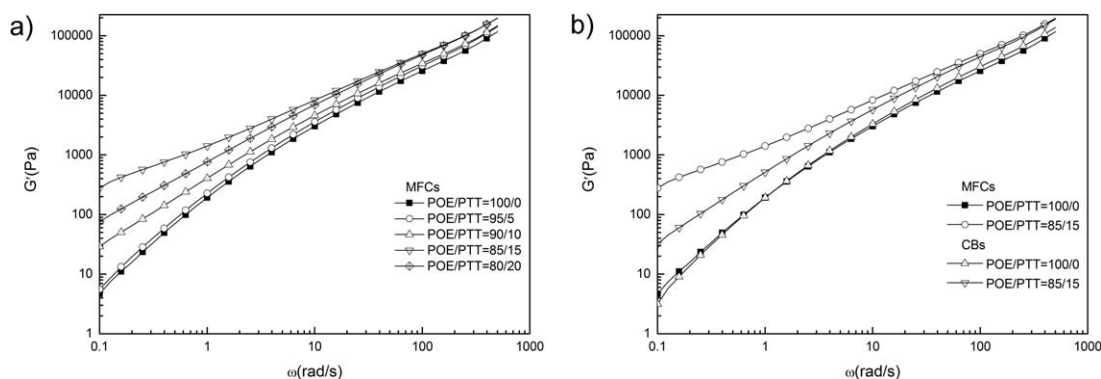


Figure 8. Storage modulus (G') values of POE/PTT composites: (a) different weight ratios of POE/PTT; (b) different processing methods of POE/PTT.

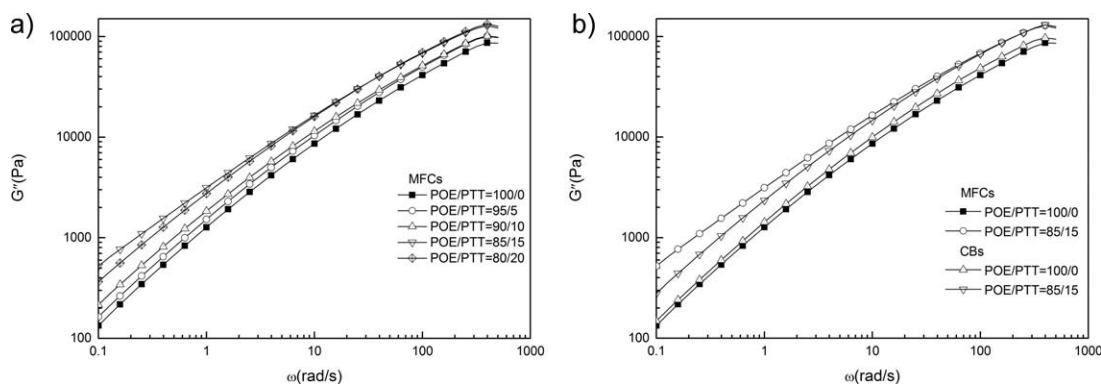


Figure 9. Loss modulus (G'') values of POE/PTT composites: (a) different weight ratios of POE/PTT; (b) different processing methods of POE/PTT.

which PET microfibrils having suitable stretch ratios (stretch ratios 5 and 8) restricted the relaxation of the PP matrix. This phenomenon indicates that there is a physical network between the solid PTT microfibrils and the molten POE matrix that can hinder the POE phase relaxation. As shown in Figure 10(b), at the same component ratio (85/15), the $\tan \delta$ values of the MFCs is lower than that of the CBs, which can prove that the PTT particles are incapable of influencing the relaxation mechanism of the POE.

Figure 11 shows the curves of the complex viscosity (η^*) versus angular frequency (ω) of the MFCs at 200 °C. The complex viscosities of all the specimens are reduced with the rise in fre-

quency. The results prove that the flowability of the system obeyed the law of a pseudoplastic fluid, which was similar to the iPP/PA6 blend.²¹ Generally, the absolute value of complex viscosity ($|\eta^*|$) is defined as follows:

$$|\eta^*| = \sqrt{(G'/\omega)^2 + (G''/\omega)^2} \quad (2)$$

Therefore, the variations in the complex viscosity are directly affected by storage modulus and loss modulus, which are related to the morphology of the dispersed phase. At low frequencies ($\omega < 1$ rad/s), the complex viscosities of the POE/PTT composites are higher than that of neat POEs, and the complex viscosity reaches the maximum at the 85/15 component ratio,

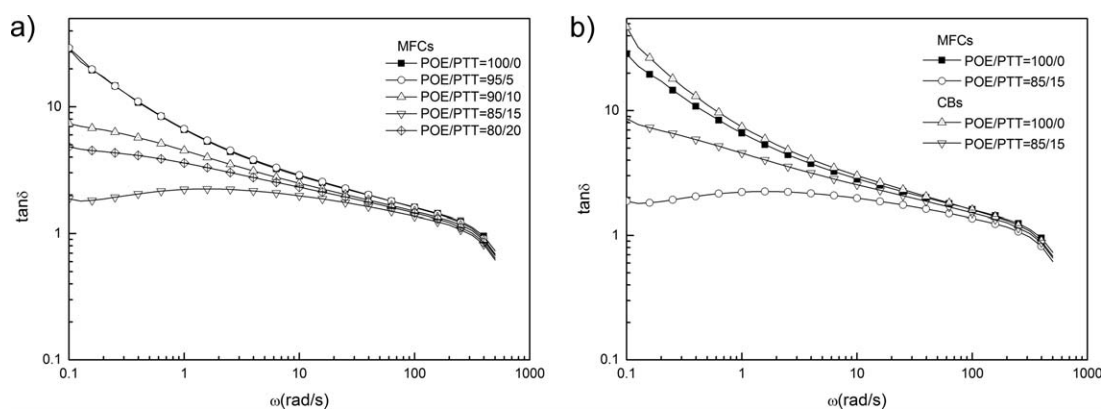


Figure 10. The $\tan \delta$ of POE/PTT composites: (a) different weight ratios of POE/PTT; (b) different processing methods of POE/PTT.

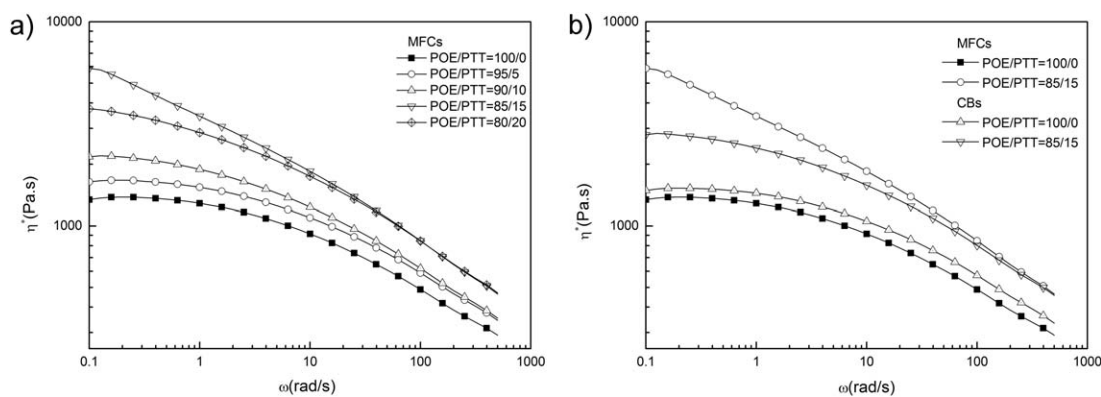


Figure 11. The complex viscosity (η^*) of POE/PTT composites: (a) different weight ratios of POE/PTT; (b) different processing methods of POE/PTT.

which implies that the presence of the PTT microfibrils hindered the mobility of the POE chain segments. The complex viscosity of MFCs is distinctly higher than that of the CBs at the same component ratio (85/15), indicating that the microfibrillar morphology of the dispersed PTT is more helpful in restricting the mobility of the POE chain segments, as shown in Figure 11(b). These results are consistent with the analyses of the storage modulus and loss modulus.

However, at high frequency ($\omega > 100$ rad/s), the differences in storage modulus, loss modulus $\tan \delta$, and complex viscosity for the different MFCs are negligible. This may be because the microfibrils are highly oriented at high frequency. Microfibrils have less chance to collide and tangle than at low frequency, where the microfibrils are disoriented. Hence, the dynamic rheology property is more sensitive to the variation of the microfibril concentration at low frequency. In contrast, the values are more similar to that of neat POE at high frequency, which indicates that the existence of the microfibrils did not impose a difficulty in processing the composites.

CONCLUSIONS

POE/PTT *in situ* microfibrillar composites are successfully prepared by multistage stretching extrusion with the assembly of LMEs. The concentration of the PTT phase influences the morphology of the PTT dispersed phase in a POE matrix during multistage stretching extrusion. SEM studies show that the number of PTT microfibrils increases with the addition of the PTT phase. When the weight ratio of POE/PTT is 85/15, the tensile strength is the highest along the extrusion direction, but when the PTT concentration is 20%, the tensile strength decreases because of the incompatibility and the scatter of the microfibril distribution. Furthermore, compared with the neat POE, the storage modulus, loss modulus, and complex viscosity are the highest while the $\tan \delta$ is the lowest for MFCs prepared at a weight ratio of 85/15, as revealed by dynamic rheology studies, especially at low frequency ($\omega < 1$ rad/s). The storage modulus values of the POE/PTT composites have more obvious changes than the loss modulus values, which is because the PTT microfibrils can form a physical network with the POE matrix and have a more significant effect on the elastic behavior than on the viscous behavior of the MFCs. Moreover, the PTT microfibrils are more useful than the PTT particles. But at high fre-

quency ($\omega > 100$ rad/s), the differences become small, indicating that the morphologies and concentration of the PTT dispersed phase in POE/PTT composites have little effect on the viscoelasticity at high frequency.

ACKNOWLEDGMENTS

The authors gratefully acknowledge the financial support of this work by the Nature Science Foundation of China (grant numbers 51363002, 51303032), the Guizhou Province Governor of Outstanding Scientific and Technological Education Personnel special funds (grant: Qian Sheng Zhuan He Zi [2012]25), the Guizhou International Science and Technology Cooperation Projects (grant: Qian Ke He Wai G Zi [2013]7044), and the Guizhou Province Guiyang Baiyun District Science and Technology Plan Projects (grant: Bai Ke He [2014]17).

REFERENCES

- Fuchs, C.; Bhattacharyya, D.; Friedrich, K.; Fakirov, S. *Compos. Interfaces* **2006**, *13*, 331.
- Huang, W.; Shen, J.; Chen, X.; Chen, H. *Polym. Int.* **2003**, *52*, 1131.
- Li, Z.; Yang, M.; Feng, J.; Yang, W.; Huang, R. *Mater. Res. Bull.* **2002**, *37*, 2185.
- Pesneau, I.; Kadi, A. A.; Bousmina, M.; Cassagnau, P.; Michel, A. *Polym. Eng. Sci.* **2002**, *42*, 1990.
- Kiss, G. *Polym. Eng. Sci.* **1987**, *27*, 410.
- Thangamathesvaran, P. M.; Hu, X.; Tam, K. C.; Yue, C. Y. *Compos. Sci. Technol.* **2001**, *61*, 941.
- Shimizu, H.; Kitano, T.; Nakayama, K. *Mater. Lett.* **2004**, *58*, 1277.
- Su, K.; Wei, K. *J. Appl. Polym. Sci.* **1995**, *56*, 79.
- Zhao, X.; Du, X.; Liu, D.; Zhou, Q. *Macromol. Mater. Eng.* **2000**, *274*, 36.
- Yin, B.; Zhao, Y.; Yang, W.; Pan, M.; Yang, M. *Polymer* **2006**, *47*, 8237.
- Mccardle, R.; Bhattacharyya, D.; Fakirov, S. *Macromol. Mater. Eng.* **2012**, *297*, 711.
- Xu, Q. W.; Man, H. C. *Polymer* **2000**, *41*, 7391.

13. Taepai boon, P.; Junkasem, J.; Dangtungee, R.; Amornsakchai, T.; Supaphol, P. *J. Appl. Polym. Sci.* **2006**, *102*, 1173.
14. Sun, X.; Yu, Q.; Shen, J.; Gao, S.; Li, J.; Guo, S. *J. Mater. Sci.* **2013**, *48*, 1214.
15. Jayanarayanan, K.; Thomas, S.; Joseph, K. *Compos. Part A: Appl. Sci. Manuf.* **2008**, *39*, 164.
16. Li, Z.; Yang, M.; Xie, B.; Feng, J.; Huang, R. *Polym. Eng. Sci.* **2003**, *43*, 615.
17. Li, Z.; Yang, W.; Xie, B.; Shen, K.; Huang, R.; Yang, M. *Macromol. Mater. Eng.* **2004**, *289*, 349.
18. Ponting, M.; Hiltner, A.; Baer, E. *Macromol. Symp.* **2010**, *249*, 19.
19. Langhe, D. S.; Hiltner, A.; Baer, E. *Polymer* **2011**, *52*, 5879.
20. Gupta, M.; Lin, Y.; Deans, T.; Baer, E.; Hiltner, A.; Schiraldi, D. A. *Macromolecules* **2010**, *43*, 4230.
21. Shen, J.; Wang, M.; Li, J.; Guo, S. *Polym. Adv. Technol.* **2011**, *22*, 237.
22. Wang, J.; Zhang, X.; Zhao, T.; Shen, L.; Wu, H.; Guo, S. *J. Appl. Polym. Sci.* **2014**, DOI: 10.1002/app.40108.
23. Yi, X.; Xu, L.; Wang, Y.; Zhong, G.; Ji, X.; Li, Z. *Eur. Polym. J.* **2010**, *46*, 719.
24. Li, Z.; Sun, C.; Li, X.; Zhang, Q.; Fu, Q. *RSC Adv.* **2015**, *104*, 85442.
25. Favis, B. D.; Chalifoux, J. P. *Polym. Eng. Sci.* **1987**, *27*, 1591.
26. Wang, D.; Sun, G. *Eur. Polym. J.* **2007**, *43*, 3587.
27. Li, M.; Xiao, R.; Sun, G. *J. Mater. Sci.* **2011**, *46*, 4524.
28. Li, Z.; Yang, W.; Xie, B.; Shen, K.; Huang, R.; Yang, M. *Macromol. Mater. Eng.* **2004**, *289*, 349.
29. Zhang, P.; Xu, D.; Xiao, R. *J. Appl. Polym. Sci.* **2015**, *132*, DOI: 10.1002/app.42184.
30. Li, M.; Xiao, R.; Sun, G. *Polym. Eng. Sci.* **2011**, *51*, 835.
31. Zhao, Z.; Yang, Q.; Xiang, Z.; Kong, M.; Tang, D.; Huang, Y.; Liao, X.; Niu, Y. *Polym. Adv. Technol.* **2015**, *26*, 1275.
32. Huang, W.; Shen, J.; Chen, X.; Chen, H. *Polym. Int.* **2003**, *52*, 1131.
33. Jayanarayanan, K.; Jose, T.; Thomas, S.; Joseph, K. *Eur. Polym. J.* **2009**, *45*, 1738.